ES cells recovered completely to the level of wild-type EB3 ES cells (Fig. 3C-E). Essentially similar inhibitory effects of Smad7 expression on mES cell propagation were observed using another clone fSmad7-7 (data not shown). Although stable expression of Smad7 interferes with mES growth, cell-cycle distribution of fSmad7-10$^+$, fSmad7-10$^-$ and EB3 ES cells was not significantly altered (data not shown). These results clearly indicate that the inhibitory effect of Smad7 on proliferation of mES cells is completely reversible.

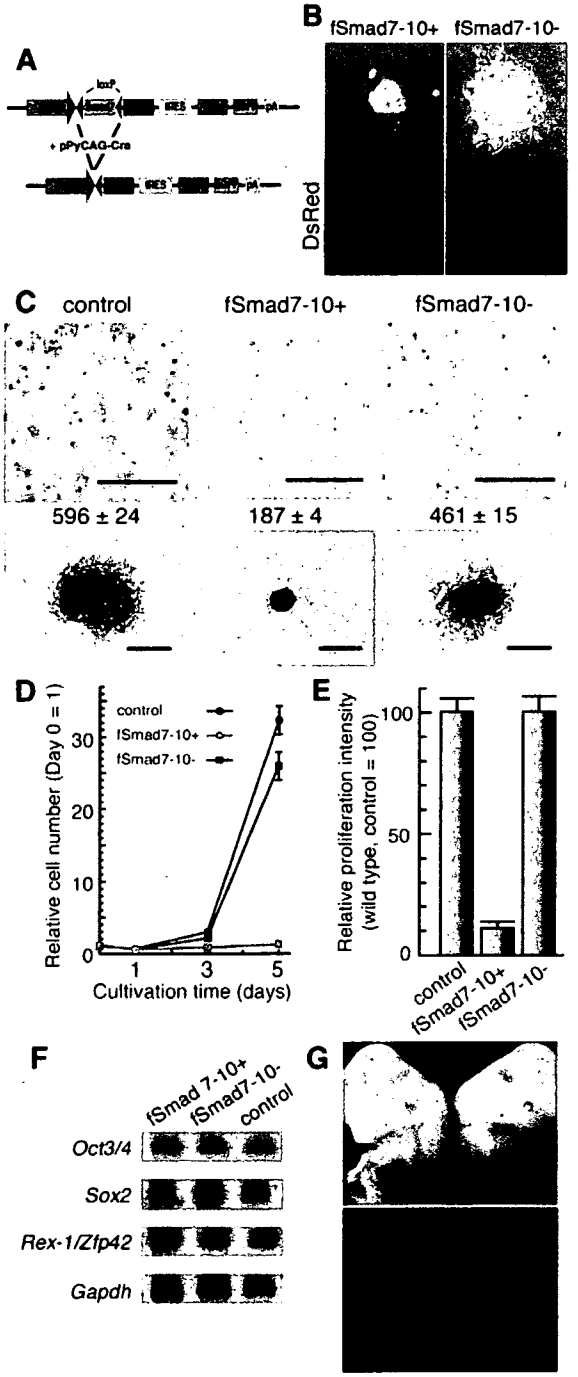

The growth-inhibitory effect of Smad7 does not affect pluripotency of mES cells

To determine whether the undifferentiated state of mES cells was retained during reversible expression of the Smad7 transgene, we prepared RNA from these ES cells and investigated the expression of three stem-cell-specific genes, *Oct3/4* (Niwa et al., 2000; Niwa et al., 2002), *Sox2* (Yuan et al., 1995) and *Zfp42/Rex1* (Rogers et al., 1991) by northern blot analysis. All stem cell marker genes were strongly expressed in both Smad7-10$^+$ and Smad7-10$^-$ ES cells (Fig. 3F) although there were differences in their expression levels (supplementary material Fig. S2). To confirm the maintenance of pluripotency in these cells, DsRed-expressing fSmad7-10$^-$ ES cells were injected into blastocysts obtained from C57BL/6 strain mice. Embryos with DsRed fluorescence were successfully obtained, suggesting that the pluripotency of Smad7-10$^-$ ES cells contributing to embryogenesis (Fig. 3G, left, compared with control littermates). These results indicate that temporary forced expression of *Smad7* does not affect the pluripotency of ES cells.

Negative effect of forced *Smad7* expression depends in part on TGFβ-related activity in FCS

We showed that activin-Nodal-TGFβ signaling is autonomously activated in ES cells in FCS-containing medium (Fig. 1A). We next examined whether this activation results from the agents included in FCS-containing medium. We recently demonstrated that ES cells, when cultured without FCS in serum-free medium supplemented with KSR, LIF, and ACTH, can propagate even from single cells (clonal density <25 cells/cm^2) with proper pluripotency (Ogawa et al., 2004). Since serum-free medium contains no TGFβ-related molecules, we used it to investigate whether the

Fig. 3. The inhibitory effect of Smad7 is reversible. (A) Strategy for generation of fSmad7-10$^+$ and fSmad7-10$^-$ ES cells. fSmad7-10$^+$ was generated by stable integration of floxed-*Smad7* cDNA transgene under the CAG promoter into EB3 ES cells. After elctroporation of pCAGGS-Cre into fSmad7-10$^+$, fSmad7-10$^-$ was free of *Smad7* cDNA and expressed DsRed. (B) Colony morphologies of fSmad7-10$^+$ (left) and Smad7-10$^-$ (right) cells. EB3 (control), fSmad7-10$^+$ and fSmad7-10$^-$ ES cells were seeded at 2000 cells/well in six-well plates, and cultured for 1 week in the medium supplemented with puromycin. The lower panel shows expression of DsRed. (C) Colony morphologies of fSmad7-10$^+$, fSmad7-10$^-$, and control ES cells. fSmad7-10$^+$ (middle), fSmad7-10$^-$ (right) and EB3 (as control, left) ES cells were cultured in FCS-containing medium for 5 days. Numbers indicate numbers of colonies appearing (n=3). The lower panel shows AP staining. Bars, 5 mm (upper panels); 200 μm (lower panels). (D) Relative numbers of each transfectant present on Days 1, 3, and 5 of culture compared with Day 0. Each bar represents the mean ± s.e.m. (n=4). (E) Relative proliferation intensity is shown as total cell number on Day 5/number of colonies appearing, compared with that of EB3 ES cells (100%). Each bar represents the mean ± s.e.m. (n=3). (F) Expression of stem cell marker genes *Oct3-4*, *Sox2*, and *Rex-1* in fSmad7-10$^+$, fSmad7-10$^-$ and EB3 (as control) ES cells examined by northern blot analysis. ES cells were cultured in FCS-containing medium for 5 days. *Gapdh* was detected as a loading control. (G) Chimeric mice derived from fSmad7-10$^-$ cells that had been cultured for at least 1 month. Chimeric mice (upper panel) expressed DsRed, whereas control mice (lower panel) exhibited no DsRed fluorescence.

negative effect of forced *Smad7* expression depends on TGFβ-related activity in FCS. In serum-free medium, although proliferation of fSmad7-10$^+$ cells was slower than that of fSmad7-10$^-$ cells and wild-type EB3 ES cells, the inhibitory effect of forced *Smad7* expression was reduced compared with that in FCS-containing medium (compare Fig. 3E with Fig. 4C). These results indicate that the growth-inhibitory effect of forced *Smad7* expression is partly due to the blockade of signaling from soluble TGFβ-related molecules in FCS that promote ES cell propagation.

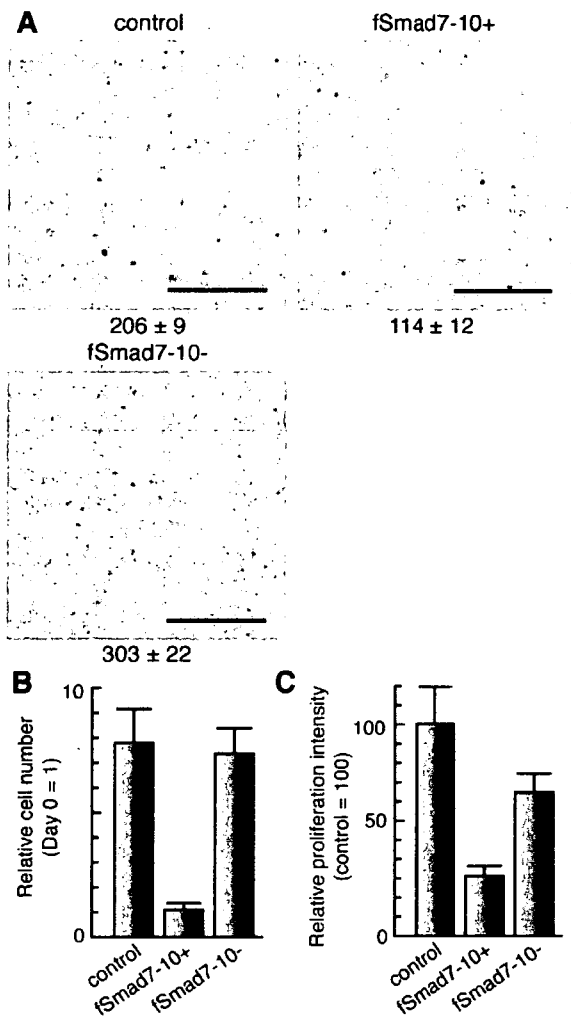

Fig. 4. Inhibitory effect of Smad7 in serum-free conditions.
(A) Colony morphologies of fSmad7-10$^+$ and fSmad7-10$^-$ ES cells in serum-free medium. fSmad7-10$^+$ (middle), fSmad7-10$^-$ (right), and EB3 (as control, left) ES cells were seeded at 2000 cells/well in six-well plates, and cultured in FCS-containing medium for 1 week. Numbers indicate numbers of colonies appearing (n=3). Bars, 5 mm. (B) Relative numbers of each transfectant present on Day 7 of culture compared with Day 0. Each bar represents the mean ± s.e.m. (n=4). (C) Relative proliferation intensity is shown as total cell number/number of colonies appearing, compared with that of EB3 ES cells (100%). Each bar represents the mean ± s.e.m. (n=3).

Exogenous Nodal and activin promote ES cell propagation in serum-free conditions

We next attempted to enhance ES cell proliferation by stimulating activin-Nodal-TGFβ signaling using exogenous ligands. To determine whether ES cells are capable of transducing TGFβ superfamily signals, we examined the expression of various TGFβ superfamily signaling components in mES cells by RT-PCR analysis (supplementary material Fig. S3). We detected transcripts of all of the TGFβ superfamily ligands except activin-βA and TGF-β3, suggesting that ES cells produce TGFβ superfamily ligands by themselves, at least at the transcriptional level. We also detected transcripts of type I and II receptors for activin-Nodal and BMPs but not ALK-7, which is known to be a specific receptor for Nodal, in MGZ5 and EB5 ES cells. However, we detected transcripts of Cripto-1 in these ES cells, suggesting that Nodal signaling can be transduced in ES cells via ALK-4 (Yan et al., 2002). By contrast, transcripts of type II TGFβ receptors were not detected, as has been previously reported (Goumans et al., 1998), suggesting that ES cells are not capable of responding to TGFβ ligands. However, transcripts of all types of Smads were detected, suggesting that ES cells are capable of responding to activin, Nodal and BMP.

We next examined whether exogenous TGFβ superfamily ligands are capable of phosphorylating Smad2 protein. When ES cells were treated with recombinant activin or Nodal for 1 hour in serum-free medium, Smad2 protein was strongly phosphorylated (Fig. 5A). By contrast, neither BMP-4 nor TGFβ phosphorylated Smad2 protein in ES cells (Fig. 5A), indicating that the TGFβ signal cannot be integrated into ES cells, as suggested above. In addition, expression of *Lefty-1* and *Lefty-2*, known target genes of Nodal (Juan and Hamada, 2001), was upregulated by treatment with recombinant Nodal (supplementary material Fig. S4), indicating that Nodal signaling was transduced into the nucleus in ES cells, as reported for other cells.

We then examined the effects of TGFβ superfamily ligands on ES cell proliferation in serum-free medium. Exogenous 30 ng/ml activin increased ES cell propagation ratio by 85% and 20% on Days 3 and 7, respectively. Furthermore, 1 or 2 μg/ml Nodal increased the ES cell propagation ratio on both Days 3 and 7 (Fig. 5B-D). Although 30 ng/ml exogenous BMP-4 appeared to slightly enhance ES cell propagation on Day 3, BMP-4 inhibited ES cell proliferation on Day 7 (Fig. 5B-D). These results suggest that activin and Nodal promote ES cell proliferation in serum-free medium via the canonical signal.

Exogenous Nodal signaling does not affect the pluripotency of mES cells

We previously found that serum-free medium supplemented with KSR and ACTH can maintain proper cellular pluripotency (Ogawa et al., 2004). In order to examine whether the undifferentiated state of ES cells was maintained when they were clonally expanded in serum-free medium supplemented with exogenous activin or Nodal, we determined the expression of ES cell markers such as *Oct3/4* (Niwa et al., 2000; Niwa et al., 2002), *Nanog* (Chambers et al., 2003; Mitsui et al., 2003), *Sox2* (Yuan et al., 1995), *Zfp42/Rex1* (Rogers et al., 1991) and *Utf1* (Okuda et al., 1998). As shown in Fig. 6A, these pluripotent state-specific genes were strongly expressed in each ES cell. To further examine the pluripotency of ES cells

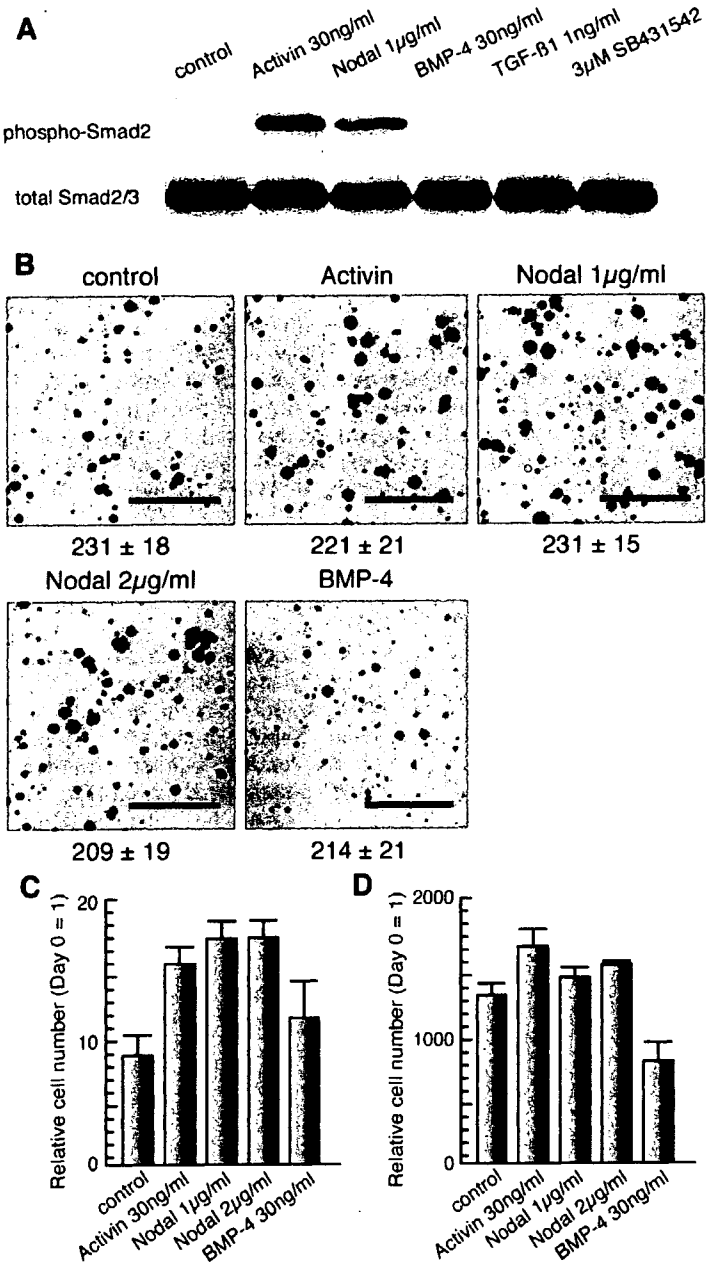

Fig. 5. Effects of TGFβ superfamily signaling on ES cell proliferation in serum-free conditions. (A) Effects of various TGFβ superfamily molecules on Smad2 phosphorylation in EB5 ES cells. EB5 cells were treated with the indicated factors for 1 hour, and subjected to western blot analysis using anti-phospho-Smad2 antibody (upper panel) and anti-Smad2/3 antibody (lower panel). (B) Colony morphologies of EB5 ES cells in serum-free medium supplemented with various TGFβ superfamily molecules. EB5 colonies were grown for 7 days in serum-free medium supplemented with no factor (as control), 30 ng/ml activin, 1 μg/ml Nodal, 2 μg/ml Nodal or 30 ng/ml BMP-4. Numbers indicate numbers of colonies appearing (n=3). Bars, 5 mm. (C,D) Relative numbers of cells treated with TGFβ superfamily molecules present on Day 3 (C) and Day 7 (D) of culture compared with that at Day 0. Each bar represents the mean ± s.e.m. (n=4).

treated with Nodal, we subcutaneously injected Nodal-treated ES cells into nude mice. These cells generated teratomas that grew to a few centimeters in size in 3-4 weeks. Histological examination revealed that they consisted of derivatives of all three germ layers, including hair-follicle-like structures with keratohyaline granules (ectoderm), cartilage (mesoderm), and ciliated or mucus-producing epithelia (endoderm) (Fig. 6B). Moreover, these cells produced overt chimeras with ES-derived agouti-chinchilla coat color (Fig. 6C). These results suggest that activin and Nodal enhance mES cell proliferation without affecting their pluripotency.

mES cells produces activin-Nodal activities for self-propagation

Although the growth-stimulatory activity of Nodal and activin was detected in serum-free medium, it was weaker than the proliferative activity inhibited by overexpression of *Smad7* or addition of SB-431542 to FCS-containing medium. To test for the presence of autocrine activin-Nodal activity, which might mask the effect of exogenous Nodal on ES cell proliferation, we performed luciferase reporter assay in serum-free medium without activin-Nodal supplementation. The relative activity of Id-1-luc was dramatically reduced in serum-free medium compared with that in FCS-containing medium (Fig. 7A). By contrast, removal of FCS resulted in the reduction of ARE-luc activity, which is consistent with the observation that Smad7 overexpression was less effective in repressing proliferation in serum-free culture, although it was less than that of Id-luc activity (Fig. 7A). We next investigated the effect of SB-431542 on ES cell proliferation in serum-free medium. Addition of 3 μM SB-431542 inhibited ES cell proliferation, as assessed by colony staining, cell number and proliferation intensity (Fig. 7B-D). The difference in proliferation ratio between fSmad7-10$^+$ and fSmad7-10$^-$ cells was less in serum-free medium than in FCS-containing medium. These results indicate that activin-Nodal signaling is autonomously activated in ES cells in serum-free conditions, and that activin-Nodal activity produced by ES cells masks the effects of exogenous Nodal or activin. Furthermore, signaling by soluble TGFβ-related molecules in FCS, presumably activin-Nodal, might increase endogenous activin-Nodal activity in ES cells.

Discussion

In the present study, we demonstrated, to our knowledge for the first time, that Nodal and activin promote mES cell proliferation with maintenance of pluripotent state in serum-free conditions. The findings presented here strongly suggest a contribution of Nodal signaling to maintenance of rapid proliferation of mES cells.

Possible roles of activin-Nodal signaling in pluripotent cell propagation during early embryogenesis

Many homozygous mutations of *Nodal*-related genes in mice result in reduction of pluripotent cell propagation

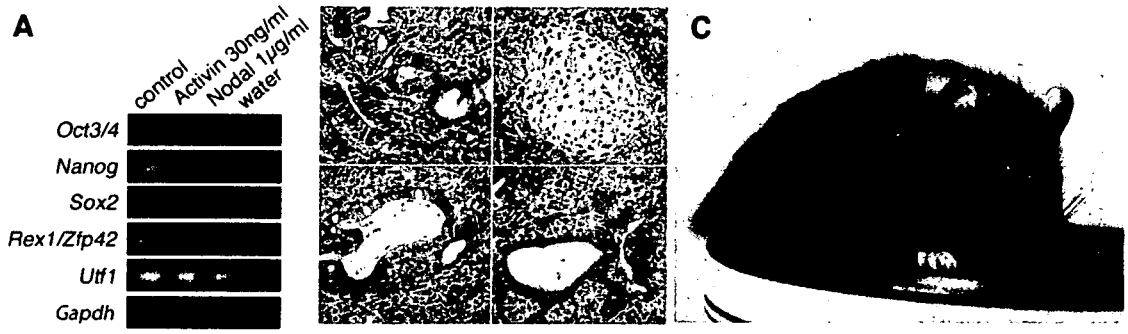

Fig. 6. Maintenance of undifferentiated state of ES cells cultured in serum-free medium with Nodal or activin. (A) Examination of expression of stem cell marker genes in EB5 ES cells clonally expanded and maintained for at least 1 month in serum-free medium supplemented with either 30 ng/ml activin or 1 μg/ml Nodal by RT-PCR analysis. *Gapdh* was detected as a loading control. (B) Hematoxylin and eosin staining of teratomas derived from EB5 ES cells cultured with Nodal protein. Tissues derived from each of the three germ layers were formed. Neuroectoderm (ectoderm; top left), cartilage (mesoderm; top right), mucus-producing epithelium (endoderm; bottom left) and ciliated epithelium (endoderm; bottom right) were observed. (C) Chimeric mouse derived from EB3 ES cells cultured with 2 μg/ml Nodal.

in early embryogenesis. ICM outgrowth is markedly reduced in *Smad4*$^{-/-}$ blastocysts (Yang et al., 1998), and the size of the epiblast cell population is substantially reduced in *Nodal*$^{-/-}$ or proprotein convertases for Nodal, *Spc1*$^{-/-}$/*Spc4*$^{-/-}$ embryos (Conlon et al., 1994; Beck et al., 2002; Robertson et al., 2003). In *Smad2*$^{-/-}$ mutant embryos, *Oct3/4* expressing regions are diminished by 8.5 days post coitus (d.p.c.), suggesting that pluripotent epiblast cells are prematurely lost (Waldrip et al., 1998). In the peri-implantation stage of the mouse embryo, the proliferation of pluripotent stem cells is tightly regulated. In the blastocyst, pluripotent stem cells exhibit very slow proliferation, with a doubling time of 64-65 hours (Copp, 1978). However, their growth accelerates after implantation, and doubling time is shortened to 11-12 hours at embryonic day 5.5 (E5.5), 9-10 hours at E6.0 and 4-5 hours at E6.5 (Snow, 1977). In serum-free medium, mES cells exhibit very slow proliferation, as pluripotent cells in ICM, at the beginning of culture, but their growth accelerates after the formation of a small colony about 5 days later (Ogawa et al., 2004). Furthermore, since the doubling time of ES cells cultured in FCS-containing medium is about 12 hours, their physiological characteristics resemble those of the epiblast around E5.0, suggesting that growth stimulation of mES cells after the formation of a small colony might correspond to the event triggering rapid epiblast growth after implantation. Interestingly, in mouse embryos, high levels of *Smad7* expression are detected during pre- and postimplantation stages when the epiblast cells are slow growing and gradually decrease from E6.5 to E7.5 while epiblast cell proliferation accelerates (Zwijsen et al., 2000), although the function of *Smad7* in mouse development has not yet been reported. These findings, together with those of the present study, suggest that the dramatic changes that occur in the proliferation of pluripotent cells during implantation stages may be regulated by Nodal, as a positive regulator, and Smad7, as a negative regulator.

Autocrine and paracrine loops of activin-Nodal signaling in ES cells

Consistent with our findings, several lines of evidence have suggested that activin-Nodal signaling is autonomously activated in human and mouse ES cells. The transcriptome of undifferentiated and differentiated hES cells was characterized to elucidate the signaling networks that play a role in the maintenance of the unique characteristics of hES cells (Brandenberger et al., 2004). These authors speculate that Nodal signaling is activated in undifferentiated hES cells, because components of Nodal signals (human orthologs of *Cripto* and *FAST1*) and a target gene (a human ortholog of *Lefty2*) are highly expressed in undifferentiated hES cells. Furthermore, phosphorylation of Smad2/3, but not of Smad1/5, was observed in undifferentiated hES cells, and decreased upon their differentiation (James et al., 2005).

We found that activin-Nodal signaling is autonomously activated in serum-free-cultured mES cells (Fig. 7), suggesting that mES cells produce activin-Nodal ligands, as supported by supplementary material Fig. S3. Notably, the target genes of Nodal include its positive regulators, such as the *Nodal* gene itself, and its negative regulators, such as *Lefty1* and *Lefty2* (Hamada et al., 2002). We failed to observe any effects of exogenous Nodal on proliferation of serum-free cultured ES cells when these cells were grown to confluence (data not shown), suggesting that Nodal ligands and/or Lefty1 and Lefty2 produced by autocrine loops of Nodal signaling in ES cells might mask the effects of exogenous Nodal or activin.

Roles of TGFβ superfamily signaling in self-renewal of ES cells

We found that exogenous addition of Nodal or activin increased mouse ES cell proliferation, whereas addition of BMP or TGFβ had no significant effects (Fig. 5B-D). The finding that TGFβ failed to affect ES cell proliferation can be explained by the lack of expression of type II receptors for TGFβ (supplementary material Fig. S3). By contrast, the failure of exogenous BMP-4 to stimulate proliferation of mES cells is inconsistent with previous reports (Ying et al., 2003a; Qi et al., 2004). BMP sustains self-renewal of mES cells in concert with LIF, and the crucial contribution of BMP to mES cell self-renewal is to induce expression of *Id* genes (Ying et al., 2003a). In N2B27 medium, which these authors used to

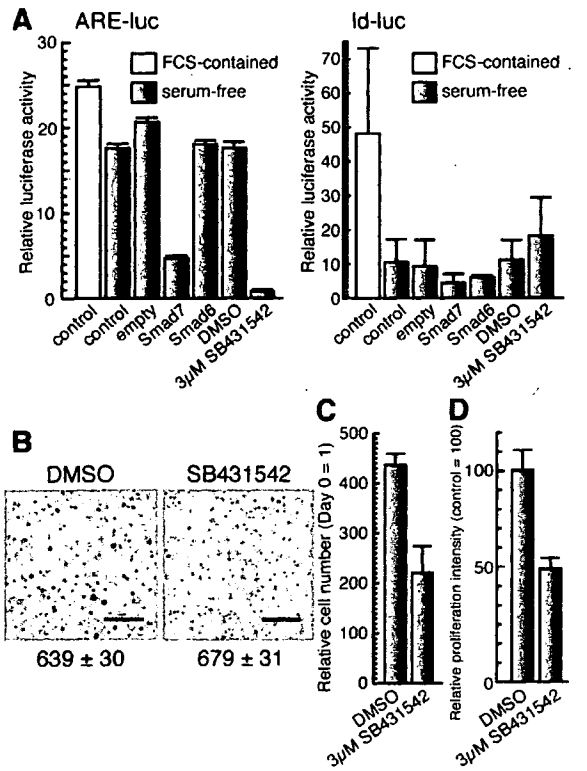

Fig. 7. ES cells produce activin-Nodal activities for self-propagation. (A) Luciferase reporter assay of MGZ5 cells with reporter constructs (ARE-luc reporter or Id-1-luc reporter). Control, cells transfected with reporter and control vectors only; Smad7, Smad6, empty, cells transfected with each expression plasmid; SB-431542, DMSO, cells cultured in medium supplemented with SB-431542 or DMSO (as control for SB-431542). Each bar represents the mean ± s.e.m. (n=3). (B) Colony morphologies of MGZ5 cells treated with SB-431542. MGZ5 cells were seeded at 2000 cells/well in six-well plates and cultured in serum-free medium supplemented with 3 μM SB-431542 (right) or DMSO (as control, left) for 1 week. Numbers indicate numbers of colonies appearing (n=3). Bars, 5 mm. (C) Relative numbers of cells treated with SB-431542 or DMSO present on Day 7 of culture compared with that at Day 0. Each bar represents the mean ± s.e.m. (n=3). (D) Relative proliferation intensity is shown as total cell number/number of colonies appearing, compared with that in cells treated with DMSO (100%). Each bar represents the mean ± s.e.m. (n=3).

test the effects of BMP, mES cells tend to differentiate into neural precursors and exhibit decreased proliferation even in the presence of LIF (Ying et al., 2003b). An autocrine BMP loop has been described in mES cells (Monteiro et al., 2004) and BMP provided by feeder cells has also been identified as a factor required for the maintenance of ES cell self-renewal (Qi et al., 2004). Since embryoid body formation studies have shown that BMP-4 inhibits neural differentiation, as found in many other vertebrate models (Wilson et al., 1995; Finley et al., 1999; Wilson and Edlund, 2001), the growth-stimulatory effects of BMP in the study by Ying et al. (Ying et al., 2003a) might have been due to its inhibitory effects on neural differentiation of mES cells intrinsically induced in serum-free conditions with N2B27 medium, in which B27 supplement contains vitamin A, a precursor of a potent differentiation inducer retinoic acid. By contrast, our serum-free culture conditions allow mES cells to maintain an undifferentiated state in the presence of LIF (Ogawa et al., 2004). To examine the possibility that endogenously activated BMP signals in our culture condition might have masked the effects of exogenous BMP-4 on mES cell proliferation, we studied the levels of Smad1/5/8 phosphorylation in the absence and presence of Noggin and BMP-4 (supplementary material Fig. S5A). Endogenous phosphorylation of Smad1/5/8 was barely detected whereas BMP-4 significantly induced their phosphorylation. While Noggin decreased Smad1/5/8 phosphorylation induced by BMP-4, it did not change the basal level of Smad1/5/8 phosphorylation, nor inhibit the mES cell propagation (supplementary material Fig. S5), suggesting that endogenous BMP signals did not play important roles under our culture conditions. We suspect that this is the reason why the present study, which focused on the effects of TGFβ superfamily members on the proliferation of undifferentiated mES cells, failed to detect growth-stimulatory effects of BMPs.

There is evidence that, during early embryogenesis, Nodal signaling plays a role in patterning of the anteroposterior body axis, formation of mesoderm and endoderm, and left-right axis patterning (Schier and Shen, 2000; Brennan et al., 2002; Eimon and Harland, 2002; Nonaka et al., 2002), suggesting that Nodal signaling induces cellular differentiation. Finding that the expression of *Zfp42/Rex-1* in Smad7-10 ES cells was higher than that in Smad7-10-1 and EB3 (supplementary material Fig. S2) suggests that endogenous activin-Nodal-TGFβ signaling might also be involved in the promotion of differentiation to primitive ectoderm of mES cells. However, in human ES cells, Nodal or activin-Nodal-TGFβ signaling plays a role in the inhibition of ES cell differentiation (Vallier et al., 2004; James et al., 2005; Beattie et al., 2005). Although addition of activin or Nodal to our serum-free medium in the absence of LIF did not significantly induce differentiation of mES cells (data not shown), it remains to be determined whether the growth-stimulatory activity of activin-Nodal signaling is associated with its potential to inhibit differentiation of mES cells.

How does Nodal signaling regulate growth and self-renewal of ES cells?

TGFβs have been shown to inhibit proliferation of many types of cells through upregulation of cell-cycle inhibitors, such as p21, p27, and p15 (Massague et al., 2000). Recently, Nodal was also shown to inhibit proliferation and induce apoptosis of human trophoblast cells through ALK7 and Smad2/3 (Munir et al., 2004). Therefore, our finding that Nodal enhances proliferation of ES cells seems exceptional. However, during formation of the anteroposterior body axis of mouse embryos, Nodal signaling provides the driving force for distal visceral endoderm (DVE) migration by stimulating the proliferation of visceral endodermal cells (Yamamoto et al., 2004), suggesting that Nodal is capable of enhancing the proliferation of certain types of cells.

To further investigate how Nodal promotes ES cell growth, we studied its effects on cell-cycle distribution and apoptosis. While activin did not affect the apoptosis of ES cells, addition of activin to ES cell culture resulted in a slight decrease in G1 ratio and subsequent increase in G2-M ratios (supplementary

material Fig. S6). The overall distribution of mES cells at different cell-cycle stages was not dramatically affected, suggesting that Nodal signaling may positively regulate the cell cycle. We examined whether the stimulation of activin or Nodal might influence the expression of *ERas*, *Utf1*, *B-Myb*, *Myc* and *CDK4*, which are reported to be components involved in propagation of mouse ES cells (Savatier et al., 1996; Iwai et al., 2001; Takahashi et al., 2003; Cartwright et al., 2005; Nishimoto et al., 2005). We found that both Nodal and activin induced a significant increase in the expression of *ERas* and *Utf1*, whereas they induced a decrease in *B-Myb* expression (supplementary material Fig. S7). Clarification of the mechanisms whereby exogenous activin-Nodal signaling regulates the propagation of mouse ES cells will require further biochemical analyses using activin- or Nodal-null ES cells in which autocrine loops of activin-Nodal signal are absent.

Various signaling cascades, such as LIF-STAT3 (Smith et al., 1988; Niwa et al., 1998; Matsuda et al., 1999) and Wnt (Sato et al., 2004; Ogawa et al., 2006), and transcription factors, such as Oct3/4 (Niwa et al., 2000; Niwa et al., 2002; Niwa et al., 2005) and Nanog (Chambers et al., 2003; Mitsui et al., 2003), are thought to play roles in the maintenance of self-renewal and/or pluripotency of ES cells. Further investigation is needed to determine the molecular mechanisms by which activin-Nodal signaling cooperates with such signaling or transcriptional networks to regulate ES cell proliferation.

We previously reported that ES cells produce an activity to support their clonal propagation in serum-free medium (Ogawa et al., 2004). Stem cell colonies were never formed from single cells in low-density culture (<100 cells/cm^2) in medium supplemented with 10% KSR and 1000 U/ml LIF (KSR medium). However, addition of a small amount (0.3%) of the final volume of FCS or 1-10 μM ACTH to KSR medium caused clonal ES cell propagation. We therefore hypothesized that a factor possessing ACTH-like activity is secreted by ES cell themselves, which we designated stem-cell autocrine factor (SAF). Since activin and Nodal enhance ES cell proliferation in an autocrine fashion, we questioned whether activin-Nodal activities mimic SAF activity. However, the addition of either activin or Nodal did not promote clonal propagation in KSR medium (data not shown), suggesting that at least two autocrine activities, those of SAF and activin-Nodal, support ES cell propagation in serum-free conditions. Based on our previous findings (Ogawa et al., 2004), we hypothesize that the survival of ES cells cultured in serum-free medium was supported by SAF activity at the start of culture, and that the growth of the attached ES cells is accelerated by upregulated autocrine Nodal signaling after cells have formed small colonies in low-density culture.

ES cells have attracted the interest of many researchers partly because of their promise for applications in regenerative medicine. However, such use requires that risks of pathogenic contamination caused by the addition of serum to medium be avoided. While the present findings obtained by mouse ES cells need to be carefully examined to be applicable for human ES cells, we hope that the combination of previously determined serum-free culture conditions and use of recombinant activin and/or Nodal will yield a safe and efficient protocol for propagation of ES cells in a completely chemically defined medium.

Materials and Methods

ES cell culture and supertransfection

MGZ5 (derived from CCE), EB5 and EB3 (derived from E14tg2a) ES cells were maintained on feeder-free, gelatin-coated plates in LIF-supplemented medium as described previously (Niwa et al., 2002). Serum-free culture medium with knockout serum replacement (KSR, Invitrogen) and 10 μM adrenocorticotrophic hormone (ACTH; American Peptides) was described previously (Ogawa et al., 2004). To assess the clonal propagation of ES cells, EB5 cells were seeded at 300 cells/well in 12-well plates and cultured in serum-free medium supplemented with various growth factors. SB-431542 (Sigma) was prepared as previously described (Watabe et al., 2003). BMP-4 (30 ng/ml), TGFβ1 (1 ng/ml), activin (30 ng/ml), Nodal (1 or 2 μg/ml) and Noggin (90 ng/ml) were purchased from R&D Systems and used in each experiment at these concentrations unless specifically noted otherwise. The colonies that appeared were stained with Leishman's reagent (Sigma) or BCIP/NBT solution (Sigma) for alkaline phosphatase staining. Transfection of episomal expression vectors [pCAG-IRESpuropA (pCAG-IP)] into MGZ5 cells (supertransfection) was performed using Lipofectamine 2000 (Invitrogen) as described previously (Niwa et al., 2002).

Generation of fSmad7-10+ and fSmad7-10- ES cells

pCAG-floxed-*DsRed*-IRES*puroEGFP* expression vector was constructed by ligation of loxP fragment, Discosoma red fluorescent protein (*DsRed*) *T4* (Bevis and Glick, 2002) expression cassette derived from pBluescript SK$^-$*DsRed T4*, and enhanced green fluorescent protein (*EGFP*) expression cassette derived from pEGFP (Clontech) into pCAG-IP. *Smad7* cDNA was introduced into the *Xho*I and *Not*I sites of pCAG-floxed-*DsRed*-IRES*puroEGFP* to obtain pCAG-f*Smad7*R-IRES*puroEGFP*.

In stable integration experiments, 2×10^7 EB3 ES cells were electroporated with 100 μg of linearized pCAG-f*Smad7*R-IRES*puroEGFP* DNA at 800 V and 3 μF in a 0.4-cm cuvette using a Gene Pulser II (Bio-Rad Laboratories) and cultured in the presence of 1 μg/ml puromycin. After 7-10 days, colonies were isolated for clonal expansion, and one of them, named fSmad7-10$^+$, was maintained in the presence of 1 μg/ml puromycin for 1 month. fSmad7-10$^-$ ES cells were generated by Cre recombination using pCAGGS-*Cre* and maintained in the presence of 1 μg/ml puromycin.

Luciferase reporter assay

MGZ5 cells were transiently transfected with an appropriate combination of reporter vector and expression plasmids together with *Renilla* luciferase control reporter vector (pTK-RL or pRL-CMV) using Lipofectamine 2000 (Invitrogen) as previously described (Chen et al., 1996; Yagi et al., 1999; Korchynskyi and ten Dijke, 2002; Kahata et al., 2004). Luciferase activities were normalized to the luciferase activity of co-transfected pTK-RL or pRL-CMV.

RNA isolation, northern blot and RT-PCR analysis

Total RNAs were prepared with ISOGEN reagent (Nippongene) or TRIzol reagent (Invitrogen) according to the manufacturer's instructions. Oligo(dT)-primed cDNAs were prepared from 1 μg of total RNA using SuperScript reverse transcriptase (Clontech) or ReverTra Ace (Toyobo). For northern blot analysis, 5 μg of total RNA were separated on a denaturing agarose gel, and then blotted onto Hybond-N membrane (Amersham Biosciences). Probes used for northern blot analyses have been previously described (Ogawa et al., 2004). Analysis was performed with GeneImage (Amersham Biosciences) according to the manufacturer's instructions. Expression of various signaling components was compared by RT-PCR analysis. PCR products were separated by electrophoresis in 1% agarose gel and visualized with ethidium bromide. Quantitative real-time RT-PCR analysis was performed using the GeneAmp 5700 Sequence Detection System (Applied Biosystems) or MyiQ Real-Time PCR Detection Systems (Bio-Rad Laboratories). Primer sequences used for PCR reactions are described in supplementary material Table S1.

Western blot analysis

Antibodies for phospho-Smad2, Smad2/3 and phospho-Smad1/5/8 for western blot analysis were obtained from Cell Signaling. Antibodies for α-tubulin were obtained from Sigma. Western blot analysis was performed as described (Kawabata et al., 1998).

Teratoma formation and generation of chimeric mouse

EB5 cells were cultured in serum-free medium supplemented with Nodal protein at clonal density for two weeks. Cells suspended in phosphate-buffered saline were subcutaneously injected into the flank of nude mice. After 3 weeks, the teratomas were excised, fixed in 10% paraformaldehyde, and subjected to histological examination with hematoxylin and eosin staining. fSmad 7-10$^-$ cells were cultured in medium supplemented with 1 μg/ml puromycin for more than 1 month. EB3 cells were cultured in serum-free medium supplemented with 2 μM recombinant Nodal at clonal density for more than 1 month. Microinjection of fSmad7-10$^-$ and EB3 ES cells into C57BL/6J blastocysts was performed according to standard procedures (Hogan et al., 1994).

Cell-cycle analysis

EB5 cells were stimulated with 30 ng/ml Activin for 24 hours. All cells (attached and detached) were collected, washed once in PBS, and the cellular DNA was stained with propidium iodide (25 μg/ml; Sigma). The cellular DNA content was analyzed by FACS (Beckman Coulter, Fullerton, CA).

We thank R. Watanabe (Kyoto University) for providing mouse *Smad6* and *Smad7* cDNAs, Tetsutaro Hayashi (RIKEN, CDB) for technical support of FACS analyses and Arisa Mita (University of Tokyo) for technical support of teratoma formation assays. This work was supported in part by a Grant Aid for Scientific Research from the Ministry of Education, Science, Culture of Japan award (to H.N. and K.M.), and Leading Project (to H.N.).

References

Beattie, G. M., Lopez, A. D., Bucay, N., Hinton, A., Firpo, M. T., King, C. C. and Hayek, A. (2005). Activin a maintains pluripotency of human embryonic stem cells in the absence of feeder layers. *Stem Cells* **23**, 489-495.

Beck, S., Le Good, J. A., Guzman, M., Ben Haim, N., Roy, K., Beermann, F. and Constam, D. B. (2002). Extraembryonic proteases regulate Nodal signalling during gastrulation. *Nat. Cell Biol.* **4**, 981-985.

Bevis, B. J. and Glick, B. S. (2002). Rapidly maturing variants of the Discosoma red fluorescent protein (DsRed). *Nat. Biotechnol.* **20**, 83-87.

Brandenberger, R., Wei, H., Zhang, S., Lei, S., Murage, J., Fisk, G. J., Li, Y., Xu, C., Fang, R., Guegler, K. et al. (2004). Transcriptome characterization elucidates signaling networks that control human ES cell growth and differentiation. *Nat. Biotechnol.* **22**, 707-716.

Brennan, J., Norris, D. P. and Robertson, E. J. (2002). Nodal activity in the node governs left-right asymmetry. *Genes Dev.* **16**, 2339-2344.

Cartwright, P., McLean, C., Sheppard, A., Rivett, D., Jones, K. and Dalton, S. (2005). LIF/STAT3 controls ES cell self-renewal and pluripotency by a Myc-dependent mechanism. *Development* **132**, 885-896.

Chambers, I., Colby, D., Robertson, M., Nichols, J., Lee, S., Tweedie, S. and Smith, A. (2003). Functional expression cloning of Nanog, a pluripotency sustaining factor in embryonic stem cells. *Cell* **113**, 643-655.

Chen, X., Rubock, M. J. and Whitman, M. (1996). A transcriptional partner for MAD proteins in TGF-beta signalling. *Nature* **383**, 691-696.

Conlon, F. L., Lyons, K. M., Takaesu, N., Barth, K. S., Kispert, A., Herrmann, B. and Robertson, E. J. (1994). A primary requirement for nodal in the formation and maintenance of the primitive streak in the mouse. *Development* **120**, 1919-1928.

Copp, A. J. (1978). Interaction between inner cell mass and trophectoderm of the mouse blastocyst. I. A study of cellular proliferation. *J. Embryol. Exp. Morphol.* **48**, 109-125.

Eimon, P. M. and Harland, R. M. (2002). Effects of heterodimerization and proteolytic processing on Derriere and Nodal activity: implications for mesoderm induction in Xenopus. *Development* **129**, 3089-3103.

Finley, M. F., Devata, S. and Huettner, J. E. (1999). BMP-4 inhibits neural differentiation of murine embryonic stem cells. *J. Neurobiol.* **40**, 271-287.

Goumans, M. J., Ward-van Oostwaard, D., Wianny, F., Savatier, P., Zwijsen, A. and Mummery, C. (1998). Mouse embryonic stem cells with aberrant transforming growth factor beta signalling exhibit impaired differentiation in vitro and in vivo. *Differentiation* **63**, 101-113.

Hamada, H., Meno, C., Watanabe, D. and Saijoh, Y. (2002). Establishment of vertebrate left-right asymmetry. *Nat. Rev. Genet.* **3**, 103-113.

Hanyu, A., Ishidou, Y., Ebisawa, T., Shimanuki, T., Imamura, T. and Miyazono, K. (2001). The N domain of Smad7 is essential for specific inhibition of transforming growth factor-beta signaling. *J. Cell Biol.* **155**, 1017-1027.

Hata, A., Lagna, G., Massague, J. and Hemmati-Brivanlou, A. (1998). Smad6 inhibits BMP/Smad1 signaling by specifically competing with the Smad4 tumor suppressor. *Genes Dev.* **12**, 186-197.

Heldin, C. H., Miyazono, K. and ten Dijke, P. (1997). TGF-beta signalling from cell membrane to nucleus through SMAD proteins. *Nature* **390**, 465-471.

Hogan, B., Beddington, R., Constantini, F. and Lacy, E. (1994). *Manipulating the Mouse Embryo.* Cold Spring Harbor, NY: Cold Spring Harbor Laboratory Press.

Imamura, T., Takase, M., Nishihara, A., Oeda, E., Hanai, J., Kawabata, M. and Miyazono, K. (1997). Smad6 inhibits signalling by the TGF-beta superfamily. *Nature* **389**, 622-626.

Inman, G. J., Nicolas, F. J., Callahan, J. F., Harling, J. D., Gaster, L. M., Reith, A. D., Laping, N. J. and Hill, C. S. (2002). SB-431542 is a potent and specific inhibitor of transforming growth factor-beta superfamily type I activin receptor-like kinase (ALK) receptors ALK4, ALK5, and ALK7. *Mol. Pharmacol.* **62**, 65-74.

Itoh, S., Landstrom, M., Hermansson, A., Itoh, F., Heldin, C. H., Heldin, N. E. and ten Dijke, P. (1998). Transforming growth factor beta1 induces nuclear export of inhibitory Smad7. *J. Biol. Chem.* **273**, 29195-29201.

Ivanova, N. B., Dimos, J. T., Schaniel, C., Hackney, J. A., Moore, K. A. and Lemischka, I. R. (2002). A stem cell molecular signature. *Science* **298**, 601-604.

Iwai, N., Kitajima, K., Sakai, K., Kimura, T. and Nakano, T. (2001). Alteration of cell adhesion and cell cycle properties of ES cells by an inducible dominant interfering Myb mutant. *Oncogene* **20**, 1425-1434.

James, D., Levine, A. J., Besser, D. and Hemmati-Brivanlou, A. (2005). TGFβ/activin/nodal signaling is necessary for the maintenance of pluripotency in human embryonic stem cells. *Development* **132**, 1273-1282.

Juan, H. and Hamada, H. (2001). Roles of nodal-lefty regulatory loops in embryonic patterning of vertebrates. *Genes Cells* **6**, 923-930.

Kahata, K., Hayashi, M., Asaka, M., Hellman, U., Kitagawa, H., Yanagisawa, J., Kato, S., Imamura, T. and Miyazono, K. (2004). Regulation of transforming growth factor-beta and bone morphogenetic protein signalling by transcriptional coactivator GCN5. *Genes Cells* **9**, 143-151.

Kawabata, M., Inoue, H., Hanyu, A., Imamura, T. and Miyazono, K. (1998). Smad proteins exist as monomers in vivo and undergo homo- and hetero-oligomerization upon activation by serine/threonine kinase receptors. *EMBO J.* **17**, 4056-4065.

Korchynskyi, O. and ten Dijke, P. (2002). Identification and functional characterization of distinct critically important bone morphogenetic protein-specific response elements in the Id1 promoter. *J. Biol. Chem.* **277**, 4883-4891.

Laping, N. J., Grygielko, E., Mathur, A., Butter, S., Bomberger, J., Tweed, C., Martin, W., Fornwald, J., Lehr, R., Harling, J. et al. (2002). Inhibition of transforming growth factor (TGF)-beta1-induced extracellular matrix with a novel inhibitor of the TGF-beta type I receptor kinase activity: SB-431542. *Mol. Pharmacol.* **62**, 58-64.

Massague, J. (1998). TGF-beta signal transduction. *Annu. Rev. Biochem.* **67**, 753-791.

Massague, J., Blain, S. W. and Lo, R. S. (2000). TGFbeta signaling in growth control, cancer, and heritable disorders. *Cell* **103**, 295-309.

Matsuda, T., Nakamura, T., Nakao, K., Arai, T., Katsuki, M., Heike, T. and Yokota, T. (1999). STAT3 activation is sufficient to maintain an undifferentiated state of mouse embryonic stem cells. *EMBO J.* **18**, 4261-4269.

Mitsui, K., Tokuzawa, Y., Itoh, H., Segawa, K., Murakami, M., Takahashi, K., Maruyama, M., Maeda, M. and Yamanaka, S. (2003). The homeoprotein Nanog is required for maintenance of pluripotency in mouse epiblast and ES cells. *Cell* **113**, 631-642.

Monteiro, R. M., de Sousa Lopes, S. M., Korchynskyi, O., ten Dijke, P. and Mummery, C. L. (2004). Spatio-temporal activation of Smad1 and Smad5 in vivo: monitoring transcriptional activity of Smad proteins. *J. Cell Sci.* **117**, 4653-4663.

Munir, S., Xu, G., Wu, Y., Yang, B., Lala, P. K. and Peng, C. (2004). Nodal and ALK7 inhibit proliferation and induce apoptosis in human trophoblast cells. *J. Biol. Chem.* **279**, 31277-31286.

Nakao, A., Afrakhte, M., Moren, A., Nakayama, T., Christian, J. L., Heuchel, R., Itoh, S., Kawabata, M., Heldin, N. E., Heldin, C. H. et al. (1997). Identification of Smad7, a TGFbeta-inducible antagonist of TGF-beta signalling. *Nature* **389**, 631-635.

Nishimoto, M., Miyagi, S., Yamagishi, T., Sakaguchi, T., Niwa, H., Muramatsu, M. and Okuda, A. (2005). Oct-3/4 maintains the proliferative embryonic stem cell state via specific binding to a variant octamer sequence in the regulatory region of the UTF1 locus. *Mol. Cell. Biol.* **25**, 5084-5094.

Niwa, H. (2001). Molecular mechanism to maintain stem cell renewal of ES cells. *Cell Struct. Funct.* **26**, 137-148.

Niwa, H., Burdon, T., Chambers, I. and Smith A. (1998). Self-renewal of pluripotent embryonic stem cells is mediated via activation of STAT3. *Genes Dev.* **12**, 2048-2060.

Niwa, H., Miyazaki, J. and Smith, A. G. (2000). Quantitative expression of Oct-3/4 defines differentiation, dedifferentiation or self-renewal of ES cells. *Nat. Genet.* **24**, 372-376.

Niwa, H., Masui, S., Chambers, I., Smith, A. G. and Miyazaki, J. (2002). Phenotypic complementation establishes requirements for specific POU domain and generic transactivation function of Oct-3/4 in embryonic stem cells. *Mol. Cell. Biol.* **22**, 1526-1536.

Niwa, H., Toyooka, Y., Shimosato, D., Strumpf, D., Takahashi, K., Yagi, R. and Rossant, J. (2005). Interaction between Oct3/4 and Cdx2 determines trophectoderm differentiation. *Cell* **123**, 917-929.

Nonaka, S., Shiratori, H., Saijoh, Y. and Hamada, H. (2002). Determination of left-right patterning of the mouse embryo by artificial nodal flow. *Nature* **418**, 96-99.

Ogawa, K., Matsui, H., Ohtsuka, S. and Niwa, H. (2004). A novel mechanism for regulating clonal propagation of mouse ES cells. *Genes Cells* **9**, 471-477.

Ogawa, K., Nishinakamura, R., Iwamatsu,Y., Shimosato, D. and Niwa, H. (2006). Synergistic action of Wnt and LIF in maintaining pluripotency of mouse ES cells. *Biochem. Biophys. Res. Commun.* **343**, 159-166.

Okuda, A., Fukushima, A., Nishimoto, M., Orimo, A., Yamagishi, T., Nabeshima, Y., Kuro-o, M., Boon, K., Keaveney, M., Stunnenberg, H. G. et al. (1998). UTF1, a novel transcriptional coactivator expressed in pluripotent embryonic stem cells and extra-embryonic cells. *EMBO J.* **17**, 2019-2032.

Qi, X., Li, T. G., Hao, J., Hu, J., Wang, J., Simmons, H., Miura, S., Mishina, Y. and Zhao, G. Q. (2004). BMP4 supports self-renewal of embryonic stem cells by inhibiting mitogen-activated protein kinase pathways. *Proc. Natl. Acad. Sci. USA* **101**, 6027-6032.

Ramalho-Santos, M., Yoon, S., Matsuzaki, Y., Mulligan, R. C. and Melton, D. A. (2002). "Stemness": transcriptional profiling of embryonic and adult stem cells. *Science* **298**, 597-600.

Raz, R., Lee, C. K., Cannizzaro, L. A., d'Eustachio, P. and Levy, D. E. (1999). Essential role of STAT3 for embryonic stem cell pluripotency. *Proc. Natl. Acad. Sci. USA* **96**, 2846-2851.

Robertson, E. J., Norris, D. P., Brennan, J. and Bikoff, E. K. (2003). Control of early anterior-posterior patterning in the mouse embryo by TGF-beta signalling. *Philos. Trans. R. Soc. Lond. B Biol. Sci.* **358**, 1351-1357.

Rogers, M. B., Hosler, B. A. and Gudas, L. J. (1991). Specific expression of a retinoic acid-regulated, zinc-finger gene, Rex-1, in preimplantation embryos, trophoblast and spermatocytes. *Development* **113**, 815-824.

Sato, N., Meijer, L., Skaltsounis, L., Greengard, P. and Brivanlou, A. H. (2004). Maintenance of pluripotency in human and mouse embryonic stem cells through activation of Wnt signaling by a pharmacological GSK-3-specific inhibitor. *Nat. Med.* **10**, 55-63.

Savatier, P., Lapillonne, H., van Grunsven, L. A., Rudkin, B. B. and Samarut, J. (1996). Withdrawal of differentiation inhibitory activity/leukemia inhibitory factor up-regulates D-type cyclins and cyclin-dependent kinase inhibitors in mouse embryonic stem cells. *Oncogene* **12**, 309-322.

Schier, A. F. and Shen, M. M. (2000). Nodal signalling in vertebrate development. *Nature* **403**, 385-389.

Schofield, R. (1978). The relationship between the spleen colony-forming cell and the haemopoietic stem cell. *Blood Cells* **4**, 7-25.

Sirard, C., de la Pompa, J. L., Elia, A., Itie, A., Mirtsos, C., Cheung, A., Hahn, S., Wakeham, A., Schwartz, L., Kern, S. E. et al. (1998). The tumor suppressor gene Smad4/Dpc4 is required for gastrulation and later for anterior development of the mouse embryo. *Genes Dev.* **12**, 107-119.

Smith, A. G., Heath, J. K., Donaldson, D. D., Wong, G. G., Moreau, J., Stahl, M. and Rogers, D. (1988). Inhibition of pluripotential embryonic stem cell differentiation by purified polypeptides. *Nature* **336**, 688-690.

Snow, M. H. L. (1977). Gastrulation in the mouse: growth and regionalization of epiblast. *J. Embryol. Exp. Morphol.* **42**, 293-303.

Takahashi, K., Mitsui, K. and Yamanaka, S. (2003). Role of ERas in promoting tumour-like properties in mouse embryonic stem cells. *Nature* **423**, 541-545.

Vallier, L., Reynolds, D. and Pedersen, R. A. (2004). Nodal inhibits differentiation of human embryonic stem cells along the neuroectodermal default pathway. *Dev. Biol.* **275**, 403-421

Viswanathan, S., Benatar, T., Rose-John, S., Lauffenburger, D. A. and Zandstra, P. W. (2002). Ligand/receptor signaling threshold (LIST) model accounts for gp130-mediated embryonic stem cell self-renewal responses to LIF and HIL-6. *Stem Cells* **20**, 119-138.

Waldrip, W. R, Bikoff, E. K., Hoodless, P. A., Wrana, J. L. and Robertson, E. J. (1998). Smad2 signaling in extraembryonic tissues determines anterior-posterior polarity of the early mouse embryo. *Cell* **92**, 797-808.

Watabe, T., Nishihara, A., Mishima, K., Yamashita, J., Shimizu, K., Miyazawa, K., Nishikawa, S. and Miyazono, K. (2003). TGF-beta receptor kinase inhibitor enhances growth and integrity of embryonic stem cell-derived endothelial cells. *J. Cell Biol.* **163**, 1303-1311.

Wilson, P. A. and Hemmati-Brivanlou, A. (1995). Induction of epidermis and inhibition of neural fate by Bmp-4. *Nature* **376**, 331-333.

Wilson, S. I. and Edlund, T. (2001). Neural induction: toward a unifying mechanism. *Nat. Neurosci.* **4**, 1161-1168.

Yagi, K., Goto, D., Hamamoto, T., Takenoshita, S., Kato, M. and Miyazono, K. (1999). Alternatively spliced variant of Smad2 lacking exon 3. Comparison with wild-type Smad2 and Smad3. *J. Biol. Chem.* **274**, 703-709.

Yamamoto, M., Saijoh, Y., Perea-Gomez, A., Shawlot, W., Behringer, R. R., Ang, S. L., Hamada, H. and Meno, C. (2004). Nodal antagonists regulate formation of the anteroposterior axis of the mouse embryo. *Nature* **428**, 387-392.

Yan, Y. T., Liu, J. J., Luo, Y., Chaosu, E., Haltiwanger, R. S., Abate-Shen, C. and Shen, M. M. (2002). Dual roles of Cripto as a ligand and coreceptor in the nodal signaling pathway. *Mol. Cell. Biol.* **22**, 4439-4449.

Yang, X., Li, C., Xu, X., and Deng, C. (1998). The tumor suppressor SMAD4/DPC4 is essential for epiblast proliferation and mesoderm induction in mice. *Proc. Natl. Acad. Sci. USA* **96**, 3667-3672.

Ying, Q. L., Nichols, J., Chambers, I. and Smith, A. (2003a). BMP induction of Id proteins suppresses differentiation and sustains embryonic stem cell self-renewal in collaboration with STAT3. *Cell* **115**, 281-292.

Ying, Q. L., Stavridis, M., Griffiths, D., Li, M. and Smith, A. (2003b). Conversion of embryonic stem cells into neuroectodermal precursors in adherent monoculture. *Nat. Biotechnol.* **21**, 183-186.

Yuan, H., Corbi, N., Basilico, C. and Dailey, L. (1995). Developmental-specific activity of the FGF-4 enhancer requires the synergistic action of Sox2 and Oct-3. *Genes Dev.* **9**, 2635-2645.

Zwijsen, A., van Rooijen, M. A., Goumans, M. J., Dewulf, N., Bosman, E. A., ten Dijke, P., Mummery, C. L. and Huylebroeck, D. (2000). Expression of the inhibitory Smad7 in early mouse development and upregulation during embryonic vasculogenesis. *Dev. Dyn.* **218**, 663-670.

Blood First Edition Paper, prepublished online February 29, 2008; DOI 10.1182/blood-2007-10-120337

Inhibition of endogenous TGF-β signaling enhances lymphangiogenesis

Masako Oka, Caname Iwata, Hiroshi I. Suzuki, Kunihiko Kiyono, Yasuyuki Morishita, Tetsuro Watabe, Akiyoshi Komuro, Mitsunobu R. Kano, and Kohei Miyazono*

Department of Molecular Pathology, Graduate School of Medicine, University of Tokyo, 7-3-1 Hongo, Bunkyo-ku, Tokyo 113-0033, Japan

*Correspondence: K. Miyazono, Department of Molecular Pathology, Graduate School of Medicine, University of Tokyo, 7-3-1 Hongo, Bunkyo-ku, Tokyo 113-0033, Japan; Phone: +81-3-5841-3345; FAX: +81-3-5841-3354; E-mail: miyazono-ind@umin.ac.jp

Short title for the running head: Lymphangiogenesis by TGF-β inhibition

Abstract

Lymphangiogenesis is induced by various growth factors, including VEGF-C. Although TGF-β plays crucial roles in angiogenesis, the roles of TGF-β signaling in lymphangiogenesis are unknown. We show here that TGF-β transduced signals in human dermal lymphatic microvascular endothelial cells (HDLECs), and inhibited the proliferation, cord formation, and migration towards VEGF-C of HDLECs. Expression of lymphatic endothelial cell (LEC) markers, including LYVE-1 and Prox1 in HDLECs, as well as early lymph vessel development in mouse embryonic stem cells in the presence of VEGF-A and C, were repressed by TGF-β, but were induced by TGF-β type I receptor (TβR-I) inhibitor. Moreover, inhibition of endogenous TGF-β signaling by TβR-I inhibitor accelerated lymphangiogenesis in a mouse model of chronic peritonitis. Lymphangiogenesis was also induced by TβR-I inhibitor in the presence of VEGF-C in pancreatic adenocarcinoma xenograft models inoculated in nude mice. These findings suggest that TGF-β transduces signals in LECs and plays an important role in the regulation of lymphangiogenesis in vivo.

Introduction

Transforming growth factor-β (TGF-β) is a multifunctional cytokine, which regulates the growth, differentiation, migration, adhesion, and apoptosis of various types of cells. TGF-β binds to two different types of serine-threonine kinase receptors, known as type II (TβR-II) and type I (TβR-I).[1-3] Upon ligand binding, TβR-II transphosphorylates TβR-I, which in turn transmits specific intracellular signals. The type I receptors phosphorylate receptor-activated Smads (R-Smads), and induce complex formation between R-Smads and common-partner Smad (co-Smad). The R-Smad/co-Smad complexes accumulate in the nucleus, where they regulate transcription of target genes, including plasminogen activator inhibitor-1 (PAI-1) and Smad7, through interaction with various transcription factors and transcriptional coactivators. Smad2 and Smad3 are R-Smads activated by TβR-I, while Smad4 is the only co-Smad in mammals shared with the TGF-β family signaling pathways. Smad7 is an inhibitory Smad, which interacts with activated TβR-I, and interferes with the phosphorylation of R-Smads by TβR-I.

TGF-β inhibits the growth and migration of blood vascular endothelial cells in vitro, while it induces angiogenesis in vivo.[4] Mice lacking certain components of TGF-β signaling, e.g. TGF-β1, TβR-II or TβR-I, exhibit abnormalities in blood vascular tissues.[5-7] We have recently shown that inhibition of TGF-β signaling by low-dose TβR-I inhibitor decreases the coverage of endothelium by pericytes, promoting leakiness of tumor blood vessels.[8] In tumor microenvironments, TGF-β signaling has also been reported to inhibit immune function and induce deposition of extracellular matrix proteins, inducing progression of tumors in advanced cancers.[9] However, the relationship between TGF-β signaling and lymphangiogenesis has not been determined.

Various growth factors have been reported to be involved in lymphangiogenesis.

These include vascular endothelial growth factor (VEGF)-C, D, hepatocyte growth factor and angiopoetin-1 and -2.[10-15] Neo-lymphangiogenesis has also been reported to be induced by receptor tyrosine kinases, e.g. fibroblast growth factor receptor 3 (FGFR3) and platelet-derived growth factor receptor (PDGFR)-β.[13,16] Among members of the VEGF family, VEGF-A transmits signals through the tyrosine kinase receptors VEGF receptor-2 (VEGFR2) and VEGFR1, which mediate signals that are required for vasculogenesis and hematopoiesis.[17,18] VEGF-C and VEGF-D bind to VEGFR3 expressed on lymphatic vessels, and mediate signals to LECs, although they also bind to VEGFR2.[19] Analysis of *Vegfc*-null mice has revealed that VEGF-C is essential for normal development of the lymphatic vessels.[20] Moreover, VEGF-C has been found to be expressed in various human cancers, and to induce tumor metastasis through induction of angiogenesis and lymphangiogenesis.[21,22] VEGF-D also promotes metastatic spread of tumors through induction of lymphangiogenesis.[11]

Among transcription factors, Prox1, a homeobox transcription factor, has been well known as an important regulator of lymphangiogenesis. During embryonic development, LECs arise by sprouting from the cardinal veins, and migrate towards VEGF-C to form the primary lymphatic plexus.[23] Prox1 is expressed in a subset of endothelial cells of the cardinal vein during embryonic development, and these cells sprout to form the primary lymphatic plexus.[24,25] In *Prox1*-null mice, migration of LECs from the veins is arrested, leading to a complete absence of the lymphatic vasculature. Prox1 induces the expression of various LEC markers, including VEGFR3, LYVE-1, podoplanin, and integrin α_9, and represses that of blood vascular endothelial cell markers, e.g. VEGFR2 and VE-cadherin, in endothelial cells.[26-28]

In the present study, we show that TGF-β regulates the growth, migration, and cord

formation of human dermal lymphatic microvascular endothelial cells (HDLECs) in vitro. In addition to inhibiting the proliferation and migration of HDLECs, TGF-β signaling suppressed the expression of LEC-related genes, including Prox1 and LYVE-1, in these cells. Moreover, inhibition of endogenous TGF-β signaling induced early lymph vessel development in mouse embryonic stem (ES) cells, and enhanced lymphangiogenesis in a mouse chronic peritonitis model and pancreatic cancer xenograft models. The present findings suggest that endogenous TGF-β signaling negatively regulates lymphangiogenesis in inflammatory tissues as well as in certain tumor tissues.

Materials and methods

Cell culture and reagents

HDLECs were obtained from Cambrex (Walkersville, MD), and cultured in EGM2-MV medium containing endothelial cell growth supplements with 5% fetal bovine serum (FBS) (Cambrex). The murine ES cell line R1 (a kind gift of A. Nagy, Mount Sinai Hospital, Canada)[29], was cultured on mitomycin C-arrested mouse embryonic fibroblasts (Chemicon International, Temecula, CA) in stem cell medium (Knock-out DMEM, Invitrogen, Carlsbad, CA) supplemented with 15% FBS, 2 mM L-glutamine (Invitrogen), 0.1 mM 2-mercaptoethanol (Invitrogen), 0.1 mM MEM non-essential amino-acids (Invitrogen), 50 U/ml penicillin-streptomycin (Invitrogen), and 1000 U/ml leukemia inhibitory factor (Chemicon International), and passaged every 48 h. Inflammatory macrophages were collected from ascites fluid in BALB/c mice four days after induction of peritonitis by intraperitoneal injection of thioglycollate (Enriched Thioglycollate Medium, 2 ml; Becton Dickinson, Franklin Lakes, NJ). BxPC3 and MIA PaCa-2 human pancreatic adenocarcinoma

cell lines were obtained from the American Type Culture Collection (Manassas, VA). BxPC3 cells were grown in RPMI 1640 supplemented with 10% FBS. MIA PaCa-2 cells were grown in DMEM with 10% FBS. Overexpression of VEGF-C in BxPC3 cells and that of TGF-β1 in MIA PaCa-2 cells were done using a lentiviral infection system (a kind gift from H. Miyoshi, RIKEN, Tsukuba, Japan). cDNA encoding VEGF-C,[30] active form of TGF-β1,[31] or green fluorescent protein (GFP) was inserted into the multicloning site of the lentiviral vector construct, pCSII-CMV-RfA, using pENTR according to standard protocol (Invitrogen). TβR-I inhibitors LY364947 and SB431542 were purchased from Calbiochem (La Jolla, CA; Cat. No. 616451) and Sigma (St. Louis, MO; Cat. No. S-4317), respectively. LY364947 was used as a TβR-I inhibitor, unless specifically described. TGF-β1 and TGF-β3 were purchased from R&D Systems (Minneapolis, MN). Cycloheximide was from Sigma. VEGF-A and VEGF-C were purchased from R&D Systems (Cat. No. 293-VE) and Calbiochem (Cat. No. 676476), respectively.

Antibodies

Antibodies to LYVE-1, Prox1, and podoplanin were purchased from Abcam (Cambridge, UK), Chemicon International, and Research Diagnostic Inc. (Flanders, NJ), respectively. PECAM1 antibody and Mac-1 antibody were from BD Pharmingen (Franklin Lakes, NJ). Rat anti-mouse LYVE-1 antibody was a kind gift from Y. Oike and T. Suda (Keio University, Tokyo, Japan). Antibody to phospho-Smad2 was a kind gift from A. Moustakas and C.-H. Heldin (Ludwig Institute for Cancer Research, Uppsala, Sweden). Antibodies to Smad2/3 and tubulin were from BD Transduction Laboratories (Franklin Lakes, NJ) and Sigma, respectively. Alexa488- and Alexa594-conjugated secondary antibodies, and TOTO-3 were purchased from Invitrogen Molecular Probes (Eugene, OR).

Immunoblotting

Cultured cells were lysed in a buffer containing 50 mM Tris-HCl, pH 8.0, 150 mM NaCl, 1% Nonidet P-40 (Nacalai Tesque, Kyoto, Japan), 5 mM EDTA, 0.5% deoxycholic acid sodium salt-monohydrate (Nacalai Tesque), 0.1% sodium dodecyl sulfate (SDS, Nacalai Tesque), 1% aprotinin (Mitsubishi Pharma, Osaka, Japan), and 1 mM phenylmethylsulfonyl fluoride (Sigma). The cell lysates were boiled in SDS sample buffer (100 mM Tris-HCl, pH 8.8, 0.01% bromophenol blue, 36% glycerol, 4% SDS, 10 mM dithiothreitol) and subjected to SDS-PAGE. Proteins were electrotransferred to PALL FLUOROTRANS® W membranes (PALL, East Hills, NY), immunoblotted with antibodies, and detected using an ECL detection system (Amersham Pharmacia Biotech, Piscataway, NJ).

Immunostaining

Cultured cells were fixed in iced 1:1 acetone-methanol solution and incubated with antibody to Prox1 overnight at 4°C. Subsequently, cells were incubated with Alexa488-conjugated secondary antibodies (Invitrogen Molecular Probes) for 1 h at room temperature and stained with TOTO-3 for nuclear staining. Frozen sections were briefly fixed with Mildform 10N (WAKO, Osaka, Japan), and incubated with anti-LYVE-1, anti-Prox1, or anti-podoplanin antibodies. Subsequently, samples were incubated with secondary antibodies, and stained with TOTO-3 for nuclear staining. Stained cells and frozen sections were observed with a confocal microscope (Model LSM510 META; Carl Zeiss MicroImaging, Inc.). Images were imported into Adobe Photoshop and analyzed using ImageJ software (National Institutes of Health, MD).

Enzyme-linked immunosorbent assay (ELISA)

Expression levels of TGF-β1 protein were determined using TGF-β1 human ELISA kit Quantikine 2nd Generation (R&D Systems), according to manufacturer's protocol. TGF-β3 at 1 ng/ml was used as the exogenous TGF-β ligand to avoid complication in detection of TGF-β1 by ELISA. Induction of TGF-β1 in HDLECs was similar between TGF-β1 and TGF-β3 at 1 ng/ml.

RNA isolation and quantitative RT-PCR

Total RNAs from HDLECs were extracted using the RNeasy Mini Kit (QIAGEN). First-strand cDNAs were synthesized using the Quantitect Reverse Transcription kit (QIAGEN) with random hexamer primers. Quantitative real-time RT-PCR analysis was performed using the 7500 Fast Real-Time PCR System (Applied Biosystems). The primer sequences used were as follows: human GAPDH: forward 5′-GAAGGTGAAGGTCGGAGTC-3', reverse 5'-GAAGATGGTGATGGGATTTC-3', human Prox1: forward 5′-CCCAGGACAGTTTATTGACCG-3', reverse 5′-GGTTGTAAGGAGTTTGGCCCA-3', human LYVE-1: forward 5′-AGCCTGGTGTTGCTTCTCACT-3', reverse 5′-GGTTCGCCTTTTTGCTCACA-3', human Smad7: forward 5′-CCTTAGCCGACTCTGCGAACTA-3', reverse 5'-CCAGATAATTCGTTCCCCCTGT-3', human PAI-1: forward 5′-GGCTGACTTCACGAGTCTTTC-3', reverse 5'-GCGGGCTGAGACTATGACA-3', human TGF-β1: forward 5'-AGTGGACATCAACGGGTTCAG-3', reverse 5'-CATGAGAAGCAGGAAAGGCC-3', human TGF-β2: forward 5'-CTGTCCCTGCTGCACTTTTGTA-3', reverse 5'-TGTGGAGGTGCCATCAATACCT-3', human TGF-β3: forward

5'-TGGAAGTGGGTCCATGAAACCTA-3', reverse 5'-GATGCTTCAGGGTTAAGAGTGTTG-3', and human/mouse VEGF-C: forward 5'-TTCCTGCCGATGCATGTCTAA-3', reverse 5'-TGTTCGCTGCCTGACACTGT-3'.

Cell growth and cord formation assays

HDLECs (2 x 10^3 cells) were seeded in 96-well plates, and cell growth was quantified for 2 days by WST-1 assay (Nacalai Tesque) according to manufacturer's protocol. Formation of cord-like structures was determined in three-dimensional gel assays, where 1 x10^4 cells were mixed with type I-A collagen gel (Nitta Gelatin, Osaka, Japan) and seeded onto culture-slide. The formation of cord-like structures was examined using video microscopy for 3 days. At the end of observation, the lengths of the cord-like structures were quantified in the three-dimensional assay as follows: 4 microscopic fields with 5 Z-axis planes in each condition were photographed, and the total lengths of cord-like structures were quantified as the mean of the sum of the lengths in the 5 planes in each of the 4 microscopic fields. Long-running video microscopy analysis of living cells on the 8-well culture slides (BD Falcon) was performed using a Leica DM IRB microscope equipped with a hardware-controlled motor stage. The video images were analyzed using ImageJ software. For quantification of images, eight to ten fields were evaluated for each mouse.

Cell migration assay

Migration of HDLECs was determined using a Boyden chamber (8 μm pore size, BD Biosciences) with type I collagen coat. HDLECs (5 x10^4) were seeded in serum-free medium containing 0.2 % BSA in the upper chamber. VEGF-C (50 ng/ml) was added as the chemoattractant to the lower chamber, while TGF-β1 at 1 ng/ml or TβR-I inhibitor at 3 μM

was added to the upper chamber. After 6-h incubation, cells in the upper chamber were carefully removed using cotton buds and cells at the bottom of the membrane were fixed and stained with 0.5% crystal violet in 20% methanol. Quantification was performed by counting the stained cells in triplicate.

Three-dimensional collagen assays of mouse ES cells

Three-dimensional collagen assays using mouse ES cells were performed as described previously.[32,33] Briefly, R1 ES cells were trypsinized, resuspended in stem cell medium without leukemia inhibitory factor supplemented with 30 ng/ml VEGF-A at day 0. The cells were then cultured in drops hanging. After 4 days, when ES cells aggregated to form embryoid bodies, drops were collected and embryoid bodies were seeded on a layer of solidified collagen type I solution (Nitta Gelatin), and a second layer of collagen solution was added on top. After 3 h, medium with or without 30 ng/ml VEGF-A and 30 ng/ml VEGF-C was added. Medium containing VEGF-A and C was replaced every second day. TβR-I inhibitor at 3 μM or TGF-β1 at 1 ng/ml was added every second day for one week, started from one week after seeding. After culturing for two weeks, whole-mount samples were incubated with anti-LYVE-1, anti-PECAM1, anti-Prox1 and Alexa-conjugated secondary antibodies overnight. Samples were examined using a Zeiss LSM510 Meta confocal microscope for immunohistochemistry. Quantification of LYVE-1 stained areas was performed in 5 fields on 3 embryoid bodies.

Chronic peritonitis model

BALB/c mice of 4–5 weeks of age were obtained from Sankyo Laboratory (Tokyo, Japan). All animal experimental protocols were performed in accordance with the policies of the

Animal Ethics Committee of the University of Tokyo. Chronic peritonitis was induced by 5% thioglycollate. Thioglycollate (2 ml) and TβR-I inhibitor (LY364947, 1 mg/kg) were administered intraperitoneally to BALB/c mice 3 times a week. After injections of these reagents into mice for 2 weeks, the mice were sacrificed and the diaphragms were excised, fixed with Mildform 10N for 1 h at room temperature, and washed with sucrose buffer (dissolved in 1 x PBS). Whole-mount samples were subsequently incubated with anti-LYVE-1, anti-Mac-1 and Alexa594-conjugated secondary antibodies overnight. Samples were examined using a Zeiss LSM510 Meta confocal microscope for immunohistochemistry.

Cancer xenograft models

BALB/c nude mice of 5–6 weeks of age were obtained from CLEA Japan (Tokyo, Japan) and Sankyo Laboratory. Parental, or VEGF-C- or TGF-β1-expressing tumor cells (5 x10^6) in 100 μl of PBS were implanted subcutaneously into male nude mice and allowed to grow for 2–3 weeks to reach proliferative phase, before initiation of TβR-I inhibitor administration. TβR-I inhibitor LY364947, dissolved in 5 mg/ml in DMSO and diluted with 100 μl of PBS, or the vehicle control, was injected intraperitoneally at 1 mg/kg, 3 times a week for 3 weeks. Excised samples were directly frozen in dry-iced acetone for immunohistochemistry. Frozen samples were further sectioned at 10-μm thickness in a cryostat, and subsequently incubated with primary and secondary antibodies as described above. Samples were observed using a confocal microscope.

Results

TGF-β transduces signals in HDLECs

To study the effects of TGF-β on lymphangiogenesis, we first examined whether TGF-β transduces signals in HDLECs.[34] Specific small molecule inhibitors of TGF-β family type I receptor kinases ALK-4, -5, and 7 (TβR-I inhibitors, LY364947 and SB431542[35,36]) were used to suppress endogenous TGF-β family signaling. Immunoblot analysis using phospho-Smad2 antibody revealed weak phosphorylation of Smad2 in untreated HDLECs, and that 1 ng/ml of TGF-β1 enhanced the phosphorylation of Smad2 in these cells (Fig. 1A). In contrast, 3 μM of LY364947 and SB431542 decreased the basal and TGF-β1-induced Smad2 phosphorylation.

The transcription induced by TGF-β in HDLECs was further examined by quantitative real-time (RT)-PCR analysis. TGF-β1 induced transcription of Smad7 and PAI-1, and the TβR-I inhibitors strongly suppressed their transcription (Fig. 1B and C), suggesting that TGF-β transduces signals in HDLECs and TβR-I inhibitors suppress the signals induced by endogenous TGF-β. We also examined the effects of TGF-β1 (1 ng/ml) and LY364947 and SB431542 (3 μM) on proliferation of HDLECs. TGF-β1 suppressed the growth of HDLECs, while TβR-I inhibitors enhanced their proliferation in the presence and absence of TGF-β1 (Fig. 1D and data not shown). These findings indicate that HDLECs respond to TGF-β signals similarly to human umbilical vein endothelial cells (HUVECs) (Supplementary Fig. S1).

Next, production of TGF-β by HDLECs was examined at mRNA and protein levels. TGF-β induced the expression of TGF-β1 mRNA, while the TβR-I inhibitors suppressed it in the presence and absence of TGF-β1 (Fig. 1E). Expression of TGF-β2 or TGF-β3 mRNA was not significantly suppressed by the TβR-I inhibitors (Supplementary Fig. S2). Moreover, ELISA revealed that HDLECs produce TGF-β1 protein at a level similar to that produced by HUVECs, and the secretion of TGF-β1 was stimulated and suppressed by exogenous TGF-β